Electronic structure and f-orbital occupancy in Yb-substituted $CeCoIn_5$

C. H. Booth,[1] T. Durakiewicz,[2] C. Capan,[3,*] D. Hurt,[3] A. D. Bianchi,[4] J.J. Joyce,[2] and Z. Fisk[3]

[1] *Chemical Sciences Division, Lawrence Berkeley National Laboratory, Berkeley, California 94720, USA*
[2] *Condensed Matter and Thermal Physics Group, Los Alamos National Laboratory,MS K764, Los Alamos, NM 87545*
[3] *Department of Physics and Astronomy, University of California Irvine, Irvine, CA 97697-4575*
[4] *Department de Physique, Universite de Montreal, Montreal H3C 3J7 Canada*

(Dated: DRAFT: Tuesday 3rd May, 2011, 09:12)

The local structure and $4f$ orbital occupancy have been investigated in $Ce_{1-x}Yb_xCoIn_5$ via Yb L_{III}-edge extended x-ray absorption fine structure (EXAFS), Ce and Yb L_{III}-edge x-ray absorption near-edge structure (XANES), and angle-resolved photoemission spectroscopy (ARPES) measurements. Yb(III) ($4f^{13}$) is the hole analog of Ce(III) ($4f^1$). Yb is found to be strongly intermediate-valent in $Ce_{1-x}Yb_xCoIn_5$ throughout the entire doping range, including pure $YbCoIn_5$, with an f-hole occupancy for Yb of $n_f \simeq 0.3$ (*i.e.* $Yb^{2.3+}$), independent of Yb concentration and independent of temperature down to $T = 20$ K. In contrast, the f-electron orbital occupancy for Ce remains close to 1 for all Yb concentrations, suggesting that there is no mutual influence on n_f between neighboring Ce and Yb sites. Likewise, ARPES measurements at 12 K have found that the electronic structure along $\Gamma - X$ is not sensitive to the Yb substitution, suggesting that the Kondo hybridization of Ce f electrons with the conduction band is not affected by the presence of Yb impurities in the lattice. The emerging picture is that in $Ce_{1-x}Yb_xCoIn_5$ there are two networks, interlaced but independent, that couple to the conduction band: one network of Ce ions in the heavy-fermion limit, one network of Yb ions in the strongly intermediate-valent limit. The robustness of the local and electronic structure to doping suggests the absence of charge transfer between the Ce and Yb ions, and may explain the relative robustness of superconductivity for this Ce-site substitution as compared to the In-site substitution.

PACS numbers: 72.15.Qm, 61.05.cj, 71.23.-k, 71.27.+a

I. INTRODUCTION

Local moment formation is ubiquitous in bulk metals and semiconductors doped with impurities containing d or f electrons, as well as in quantum dots. An impurity electron in a metallic host either remains localized and has a non-zero magnetic moment or becomes part of the conduction band, depending on the magnitude of the Coulomb repulsion and how far the impurity energy lies from the Fermi level.[1] Although the underlying physics of local moment formation is well understood, the collective behavior of a lattice of local moments is less so. In the case of a lattice of f electrons, two extreme limits are known, reflecting the two solutions of the individual impurity problem: one in which the unpaired f electron at each lattice site develops a local moment and one in which all the f electrons are delocalized. The behavior of the large number of heavy-fermion[2] and intermediate-valent compounds[3] found among the Ce- and Yb-based intermetallics can be described as variations between these limits. In the heavy-fermion limit, the charge fluctuations are suppressed due to the large Coulomb repulsion, with the valence of Ce or Yb being close to 3+, and spin fluctuations prevail. Ce(III) has a single electron in its f shell and Yb(III) has 13 f electrons, only missing one to complete the f shell. For this reason, Yb is generally considered to be the hole analog of Ce. The partial or complete screening of the lattice of local moments through the Kondo interaction between f electrons and the conduction band gives rise to extremely large electronic effective masses, with or without magnetic order. Neither a single unpaired electron or f hole is the most stable configuration for the f shell, and provided that the f-level energy is close to the Fermi energy, the valence will change into Ce(IV) or Yb(II) configurations, with an empty or closed f shell. This situation is partially realized in the intermediate-valent limit, where the lattice of f electrons hybridizes with electrons on the Fermi surface, resulting in a non-integer charge on Ce and Yb ions as well as in an electronic mass close to the band mass.

Provided one could tune in a controlled way from the heavy-fermion to the intermediate-valent limit, the suppression of the heavy fermion ground state is likely to shed light on the mechanism for heavy quasi-particle formation. Doping provides one promising route towards such a crossover. For instance, substituting Ag for Cu in $YbInCu_4$ or In for Sn in $CeSn_3$ leads to a crossover from the intermediate-valent into the heavy-fermion regime.[4–6] In these cases, the substitution onto a site other than the rare-earth site drives the valence of the rare-earth toward 3+. Substitutions onto the rare-earth site have also been made, but usually with a non-magnetic analogue in order to study the cross-over between Anderson lattice and single-impurity model behavior, such as in $Yb_{1-x}Lu_xAl_3$,[7] or to introduce scattering into superconducting planes, as in $Ce_{1-x}La_xCoIn_5$.[8,9]

The focus of this article is to explore how the electronic, magnetic, and structural behavior changes when substituting onto the rare-earth site, not with a non-magnetic ion, but rather with a different rare-earth. To

this end, we report a controlled substitution of Yb into the unconventional d-wave[10] heavy-fermion superconductor (T_c = 2.3 K) $CeCoIn_5$.[11] One previous investigation of doping rare-earths,including Yb, onto the Ce site in $CeCoIn_5$ studied the effect of altering local moment interactions on changes in T_c and non-Fermi-liquid behavior.[12] In that and our previous work[13], Yb was assumed to be divalent, and would thus be in a nonmagnetic f^{14} configuration. Here we consider the possibility that Yb has a trivalent component to its configuration, since such a configuration would be nominally isoelectronic, and yet, for the reasons explained above, substituting Yb(III) for Ce(III) is expected to be equivalent to hole doping of the Ce Kondo lattice. In this way, Yb substitution into $CeCoIn_5$ is a route to study the heavy-fermion/intermediate-valent crossover behavior.

The $CeCoIn_5$ system is a good choice for substitution studies, since the stoichiometry is stable and sizeable and clean single crystals can be grown. Earlier investigations of La substitution for Ce have revealed that the coherence of the Kondo lattice is achieved through intersite coupling.[8] The importance of the Ruderman-Kittel-Kasuya-Yosida (RKKY) coupling for the Kondo-lattice coherence scale has been recently demonstrated in a variety of heavy fermion compounds.[14] A variety of rare-earth substitutions for Ce have been attempted since, revealing that the suppression of superconductivity involves an electronic inhomogeneous state, consistent with a percolation picture.[15] Here we show the Yb substitution leads to a concomitant suppression of both the T_c and the effective mass, as measured by the Sommerfeld electronic specific heat coefficient γ_0.

$CeCoIn_5$ has also attracted a lot of attention due to the possibility of tuning the ground state reversibly from superconducting to antiferromagnetic (AF) via Cd and Hg substitution for In.[16] Such quantum phase transitions are the subject of intensive investigations, both theoretically and experimentally.[17] Local structure investigations have found that Sn, Cd, and Hg substitute preferentially for In within the Ce-In plane,[18,19] helping to explain their strong pair-breaking effect on superconductivity.[16,20] However, it is less clear how such small concentrations are able to tune the ground state into an antiferromagnet. In-NQR measurements of Cd-doped $CeCoIn_5$ showed that antiferromagnetism nucleates around Cd impurities and that the two ground states coexist microscopically.[21] On the other hand, a de Haas van Alphen (dHvA) investigation of the Fermi surface evolution with Cd substitution recently showed that the f electrons remain part of the Fermi surface in the high field paramagnetic state for a doping range where a transition from superconducting to antiferromagnetic takes place at $H = 0$. This lead to the suggestion that antiferromagnetism is intermediate between local and itinerant in this system.[13]

The electronic structure of $CeCoIn_5$ has also been subject to intensive scrutiny. So far, ARPES results have shown that even at T = 20 K, which is well below the coherence temperature ($T_{\rm coh}$ = 40 K) where heavy quasiparticles form, f electrons appear to be localized, in the sense that they are not part of the Fermi surface.[22,23] In contrast, the dHvA results at much lower temperatures are quite consistent with band structure calculations involving itinerant f electrons: the extremal orbit sizes are systematically larger than in the non-magnetic La-analog.[24,25] Determining how the f electrons become part of the Fermi surface upon cooling will dramatically enhance the state of our knowledge on Kondo lattice physics.

The main conclusion presented below and supported by magnetic susceptibility, specific heat, extended x-ray absorption fine-structure (EXAFS), x-ray absorption near-edge structure (XANES), and ARPES measurements, is that $CeCoIn_5$ can be tuned from the heavy-fermion to the intermediate-valent regime with Yb substitution, *without any change in the valence of either the Ce or Yb ions*. This conclusion is demonstrated first by presenting the experimental methods in Sec. II and results in Sec. III. The implications of these results are discussed in Sec. IV, and in particular, the local electronic-structure dependence on the Yb concentration is considered in light of the Ce/Yb interactions and the relative robustness of superconductivity compared with Sn, Cd, Hg, or even La substitutions.

II. EXPERIMENTAL METHODS

Single crystals of $Ce_{1-x}Yb_xCoIn_5$ have been grown from excess In flux, as described elsewhere.[26] In particular, micrograph measurements indicate that the actual Yb concentrations deviate from the nominal concentrations for $x > 0.6$, and possibly as low as $x \approx 0.4$.[26] All x concentrations reported forthwith are nominal concentrations.

Powder diffraction data were collected in a standard $\Theta - 2\Theta$ x-ray diffractometer using a Cu target at room temperature. Si standard was used as a reference in the x-ray pattern (Rietveld) refinements. Specific heat measurements were carried out down to $T \sim 0.4$ K in a He^3 Physical Property Measurement System (PPMS) , using the standard adiabatic heat-pulse technique. Magnetic susceptibility measurements were made in a 1 kOe field (applied in the ab-plane) in a vibrating sample SQUID magnetometer down to $T \sim 1.8$ K.

X-ray absorption measurements were performed on samples with nominal Yb concentrations of x = 0.2, 0.4, 0.8, and 1.0 on beamline 11-2 at the Stanford Synchrotron Radiation Lightsource (SSRL) at both the Ce and Yb $L_{\rm III}$-edge. All data were collected in fluorescence mode using a multi-element Ge detector. In addition to using the Ge detector to measure only L_α fluorescent x-rays, the double Si(220) monochromator was detuned by 50% to reduce contributions from higher harmonic energies. Samples were prepared for these experiments by grinding them with a mortar and pestle, passing the ma-

terial through a 30 μm sieve, and then brushing the resulting powder onto adhesive tape. Twenty strips of the tape were stacked to obtain a satisfactory fluorescence signal. Dead-time corrections were applied.

EXAFS data were collected at the Yb $L_{\rm III}$ edge. These data were extracted from the absorption data, $\mu(E)$, as a function of the incident photon energy, E, using standard procedures.[27] In particular, a 7-knot cubic spline was fit through the pre-edge subtracted data, $\mu_{\rm pre}$ to determine the embedded-atom background absorption, μ_0. The EXAFS oscillations were then obtained from $\chi(k) = \mu(k)/\mu_0(k) - 1$, where the photoelectron wave vector magnitude, k, is obtained from $\hbar^2k^2/2m_e = E - E_0$, and the photoelectron threshold energy, E_0, is arbitrarily determined from the energy at the half-height of the absorption edge and is then allowed to vary in the fitting procedure. Self-absorption corrections were applied.[28] The data were fit in r-space with backscattering phases and amplitudes calculated using the FEFF7[29] code. Single-scattering paths up to the Yb-Yb path at 4.53 Å were included individually, while multiple scattering paths were fit as a unit. A single scale factor, S_0^2, was used for all scattering paths in each sample in these fits, as was a single threshold energy shift, ΔE_0. The number of neighbors was held fixed to the nominal structure. In particular, the number of Yb-Ce pairs at the lattice constant distance (~ 4.53 Å), was fixed to $4(1-x)$, and both the pair distance, R, and the mean-squared pair distance displacement, σ^2, were held fixed to the Yb-Yb values. Reported errors were determined using a Monte Carlo method.[30] Systematic errors are typically larger, less than 0.01 Å in R and 10% in σ^2 for $R \lesssim 3$ Å, and about 0.02 Å and 20% for $R \gtrsim 3$ Å, respectively.[27]

XANES data were fit using pseudo-Voigt peaks to model the absorption resonances for each valence state, *eg.* the Ce(III) and and Ce(IV) features, together with an integrated pseudo-Voigt (essentially an arctan function) at the same energy. Another pseudo-Voigt is included to account for any EXAFS oscillations that occur in the fitting range. The f-electron occupancy for Ce (or the f-hole occupancy for Yb) is obtained by taking the weighted area of the resonances, $n_f = A^{\rm Ce(III)}/(A^{\rm Ce(III)} + A^{\rm Ce(IV)})$ (or $n_f = A^{\rm Yb(III)}/(A^{\rm Yb(II)} + A^{\rm Yb(III)})$ for Yb). The effective valence is then $v = 3 + n_f$ for Ce (or $v = 2 + n_f$ for Yb).

Angle-resolved photoemission (ARPES) measurements were performed at the Synchrotron Radiation Center in Stoughton, Wisconsin, using the Plane Grating Monochromator beamline and a Scienta 4000 spectrometer. Samples were oriented by Laue diffraction prior to measurement, and data for all samples were collected along the $\Gamma - X$ direction in the Brillouin zone. Samples were cooled down to 12 K in a vacuum of 5×10^{-11} Torr and then cleaved for measurement. Overall energy and momentum resolutions were 20 meV and 0.1 Å^{-1}, respectively. The photon energy for the $CeCoIn_5$ sample was 123 eV, and for both samples with Yb, 100 eV photons were used. Choice of photon energy was dictated by previous experiences with a clear f^{14} signal at 100eV for Yb systems and the $4d$-$4f$ resonance giving a strong $4f$ signal at 123 eV in Ce systems.

III. RESULTS

Rietveld refinements of the powder x-ray diffraction (XRD) data indicate the lattice constants for the pure $YbCoIn_5$ are $a = 4.533(3)$ Å and $c = 7.413(8)$ Å, using a Si standard. The z-position fraction for the In(2) site was fixed at 0.3060, as previously measured.[31] The Yb near-neighbor pair distances for this room temperature measurement are reported in Table I.

The magnetic susceptibility and specific heat data from $YbCoIn_5$ are shown in Fig. 1 and Fig. 2. The $\chi(T)$ values are quite small, and have been previously interpreted as indicative of a Yb(II), f^{14} state. Note that the reported $\chi(T)$ includes contributions from the unfilled Co d and In p shells, as well as the core diamagnetism. The estimated linear Sommerfeld coefficient of the specific heat, $\gamma_0 = 11.6$ mJ mol^{-1} K^{-2}, is small, typical of a weakly-correlated electron system. The estimated Debye temperature infered from the T^3 coefficient to the low-temperature specific heat data is $\Theta_{\rm D} = 216(1)$ K.

The evolution of the critical temperature T_c and of the electronic specific heat coefficient γ_0 in $Ce_{1-x}Yb_xCoIn_5$ is shown as a function of the Yb concentration in Fig. 3. T_c is defined as the midpoint of the specific heat jump at zero field and γ_0 is obtained from $T = 0$ linear extrapolation of the specific heat data, $\frac{C}{T}$ vs. T, above the upper critical field at $H = 5$ T. It is very important to note that, with the exception of $YbCoIn_5$, these data are per mol-Ce. The $YbCoIn_5$ data are per mol-Yb. Both quantities are systematically suppressed with Yb doping. The suppression of T_c with doping is much slower than with In-site substitutions, as discussed below. The suppression of γ_0 confirms that the Ce Kondo lattice is diluted upon Yb substitution.

The local structure properties of $Ce_{1-x}Yb_xCoIn_5$ were investigated using EXAFS. Fit results for $x = 0.2, 0.4, 0.6, 0.8$ and 1 are given in Table I. EXAFS data and fit quality are reasonable for all measured samples (Fig. 4). The measured bond lengths are in excellent agreement with the diffraction results, although it should be noted that the EXAFS data were collected at 50 K. The measured mean-squared displacements of the bond lengths, σ^2, are also consistently small for all atom pairs and all x. The main result from this data is that there are no obvious trends associated with x, except in the overall scale factors, S_0^2. These are close to that found[32] for fits to $YbAl_3$ data, namely, $S_0^2 = 0.7$,[32] with the highest value occurring for the $YbCoIn_5$ data (0.76). However, the other samples give lower values, especially for x =0.8 and 0.4. We interpret these low values of S_0^2 as indicative of a 5-15% amorphous or disordered-substitution Yb-based impurity for $x \neq 1$. The only unusual measurements are the extremely small values of σ^2 for the Yb-Co

TABLE I. Fit results from Yb L_{III}-edge EXAFS data at 50 K in $Ce_{1-x}Yb_xCoIn_5$. Fit range is between 1.5 and 5.0 Å.The k^1-weighted data are transformed between 2.5-15.0 $Å^{-1}$ and are Gaussian narrowed by 0.3 $Å.^{-1}$ Multiple scattering contributions (not shown) are included. Fit parameters with no reported error are constrained as shown. Reported errors are determined using a Monte Carlo technique.[30] XRD pair distances, R_{XRD}, for $YbCoIn_5$are reported for comparison, although note that these are room temperature measurements.

			$x = 1.0$		$x = 0.8$		$x = 0.6$		$x = 0.4$		$x = 0.2$	
	R_{XRD}	N	$\sigma^2(Å^2)$	$R(Å)$	$\sigma^2(Å^2)$	$R(Å)$	$\sigma^2(Å^2)$	$R(Å)$	$\sigma^2(Å^2)$	$R(Å)$	$\sigma^2(Å^2)$	$R(Å)$
Yb-In(1)	3.2053	4	0.0017(1)	3.194(1)	0.0018(2)	3.201(2)	0.0018(2)	3.198(1)	0.0019(3)	3.205(2)	0.0019(2)	3.212(2)
Yb-In(2)	3.2066	8	0.0017	3.195	0.0018	3.202	0.0018	3.199	0.0019	3.206	0.0019	3.214
Yb-Co	3.7065	2	0.0000(1)	3.707(9)	0.0000(1)	3.72(1)	0.0000(1)	3.714(8)	0.0000(1)	3.72(1)	0.0000(1)	3.74(1)
Yb-Yb	4.5330	$4x$	0.002(1)	4.54(1)	0.002(1)	4.56(1)	0.003(1)	4.55(1)	0.004(2)	4.56(2)	0.002(1)	4.59(1)
Yb-Ce	-	$4(1-x)$	0.002	4.54	0.002	4.56	0.003	4.55	0.004	4.56	0.002	4.59
ΔE_0			-3.9(3)		-4.2(3)		-3.9(3)		-4.5(4)		-4.0(4)	
S_0^2			0.76(4)		0.63(3)		0.71(3)		0.61(4)		0.66(4)	
$R(\%)$			9.73		11.45		9.81		14.73		12.67	

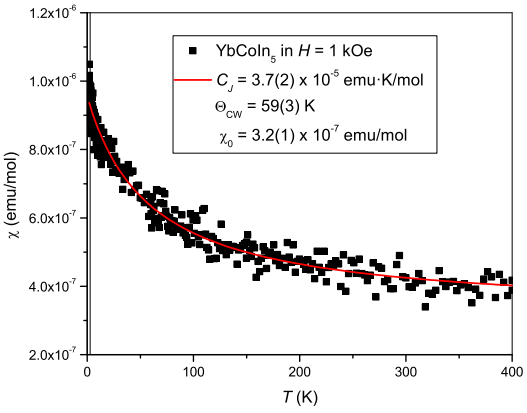

FIG. 1. (Color online) Magnetic susceptibility, $\chi(T)$, data for $YbCoIn_5$ in 1 kOe, together with fit to $\chi(T) = C_J/(T - \Theta_{CW}) + \chi_0$.

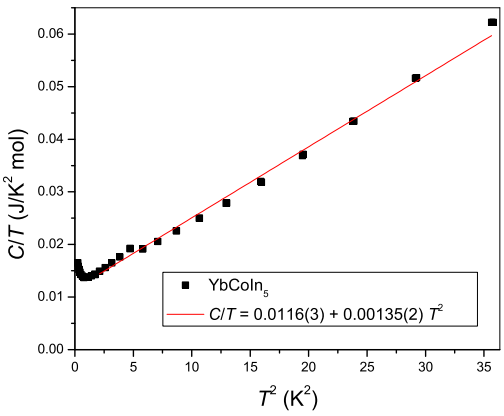

FIG. 2. (Color online) Specific heat, $C(T)$, data for $YbCoIn_5$ plotted as C/T vs. T^2, at zero field, together with a linear fit.

pairs. This peak in the EXAFS spectrum is the smallest of all the fitted peaks, since there are only 2 Yb-Co paths per Yb and Co is the weakest backscatterer in the compound. We are therefore inclined to ascribe this small value to systematic errors in the FEFF7 backscattering functions coupled with imperfect multiple scattering calculations, rather than to some actual physical property of the compounds.

Unfortunately, these data cannot be used to determine how well Yb is mixed into the $CeCoIn_5$ matrix, or the actual doping level: If the constraint on the number of Yb-Ce neighbors is released, the estimated relative error on N is about 100%.

The structural data indicate the Yb sublattice is well ordered, although some impurity phase exists for $x \neq 1$. The $R(\%)$ values are not indicative of a high-quality fit; a high-quality EXAFS fit should be near 5%. However, as seen in Fig. 4, there is no obvious misfit amplitude. Therefore, together with with the low measured values of σ^2, we conclude that the impurity phase is amorphous or highly disordered.

The valence of Ce and Yb in $Ce_{1-x}Yb_xCoIn_5$ was determined using XANES. The Ce L_{III}-edge XANES data shown in Fig. 5 are typical of a nearly trivalent-cerium intermetallic, and are consistent with previously measured Ce 115 samples.[33] The Yb L_{III}-edge data (Figs. 6 and 7), on the other hand, show a distinctly double-bumped feature indicative of a strongly intermediate-valence compound. The first feature is just below 8938 eV and is due to the Yb(II) component, and the second feature is about 8 eV higher and is due to the Yb(III) component of the Yb wavefunction. The fit results for n_f from both the Ce and Yb data are displayed in Fig. 8, representing the main conclusions of this paper. There is no observed temperature dependence (see also Fig. 6), although there is a small dependence on x (see also Fig. 7(a)). The x dependence on the f-orbital occupancy tracks the changes in S_0^2, indicating that the amorphous disordered Yb-based

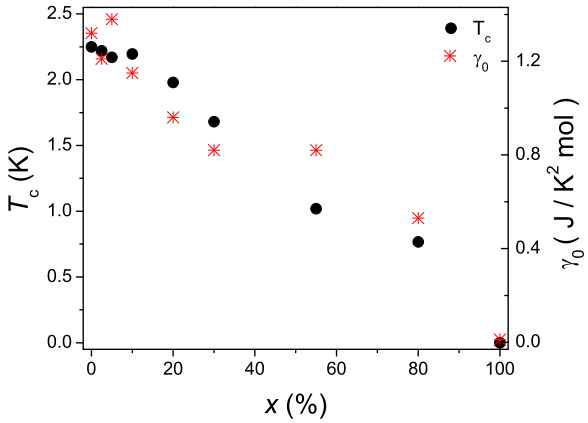

FIG. 3. (Color online) Superconducting transition temperature, T_c, as a function of Yb concentration, x, in $Ce_{1-x}Yb_xCoIn_5$. Also shown is the Sommerfeld coefficient, γ_0, determined from the T=0 linear extrapolation of C/T at $H = 5$ T (above the upper critical field). Note that, with the exception of $YbCoIn_5$, these data are per mol-Ce. The $YbCoIn_5$ data are per mol-Yb.

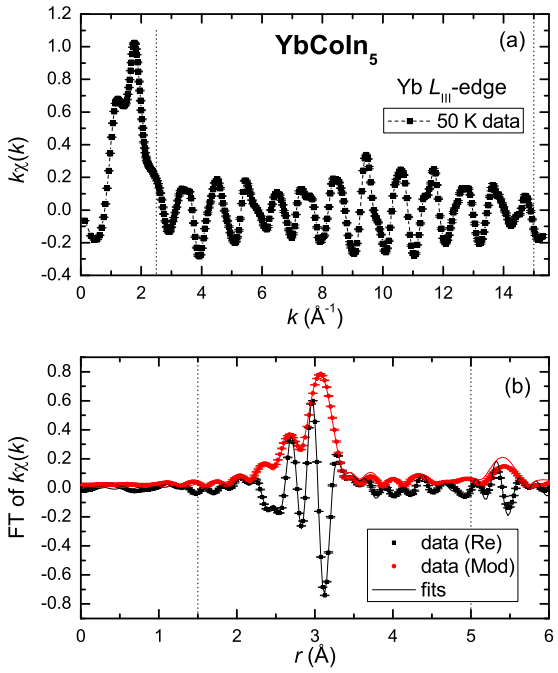

FIG. 4. (Color online) EXAFS data in both (a) k-space and (b) r-space for the Yb $L_{\rm III}$ edge on $YbCoIn_5$ as an example of data and fit quality. Error bars are based on reproducibility from multiple scans. The Fourier transform (FT) data are shown with both the real part and the modulus of the complex transform. Note that peak positions are shifted from the actual bond lengths depending on the known properties of the backscattering functions.

impurity for $x \neq 1$ is trivalent, and is therefore not elemental Yb, which is divalent. The main result of these experiments is that the valence of both Ce and Yb change little with increasing Yb concentration and/or with decreasing temperature.

We have also investigated the electronic structure in $CeCoIn_5$, $Ce_{0.91}Yb_{0.09}CoIn_5$ and $YbCoIn_5$ using ARPES. The primary task of the ARPES experiments was to look for systematic shifts within the investigated (Ce-Yb)$CoIn_5$ series, in analogy to previous ARPES experiments in $CeCoIn_5$-$CeIrIn_5$-$CeRhIn_5$. The latter shows a systematic shift of the whole band structure in connection with a ground-state transformation.[34] A small (1%) admixture of Cd on the In sites in $CeCoIn_5$ causes the electronic structure to shift down, away from the Fermi level by approximately 70 meV, while tuning the system from superconductor to antiferromagnetic. Consistently, substitution of Rh for Co, which also transforms the superconductor into an antiferromagnet, makes the f electrons more localized and results in a shift of the electronic structure by a few hundred meV. In contrast, in $Ce_{1-x}Yb_xCoIn_5$ no such shift has been detected and the electron-like d-band is found not to be sensitive to the Yb content, as seen in Fig. 9. This result is consistent with the fact that no antiferromagnetism is induced via Yb doping.

The electronic structure near the Fermi level for all three samples is comprised of two components, as shown in Figs. 9-11. One component consists of the underlying dispersive structure associated with the conduction band. This component may be clearly seen in Fig. 9, where the dispersive d-electron feature is marked by a red parabola, obtained from fitting. This dispersive band is hybridized

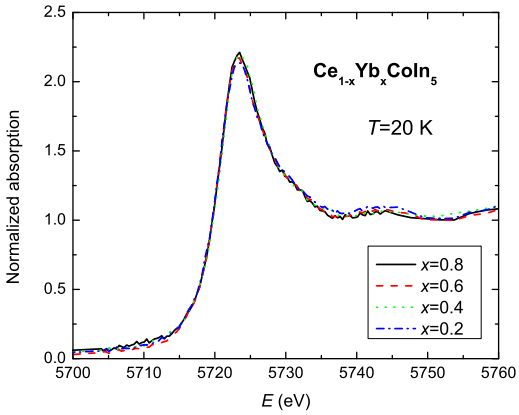

FIG. 5. (Color online) Ce $L_{\rm III}$-edge XANES data for $0.2 \leq x \leq 0.8$ from $Ce_{1-x}Yb_xCoIn_5$. Data are typical of a nearly trivalent cerium with f orbital occupancy $n_f \approx 0.9$.

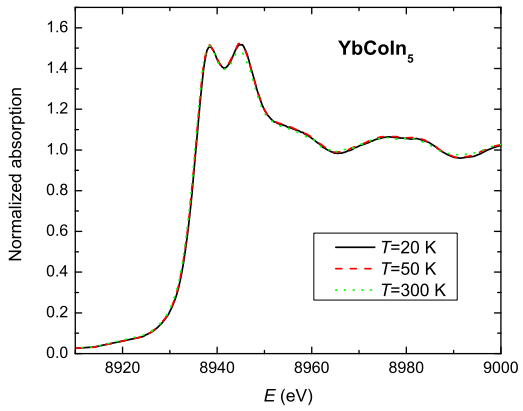

FIG. 6. (Color online) Yb $L_{\rm III}$-edge XANES data for $YbCoIn_5$ at three temperatures. A strong Yb(II) feature exists at about 8938 eV, followed by a Yb(III) feature at about 8945 eV, indicating this material is strongly intermediate valent.

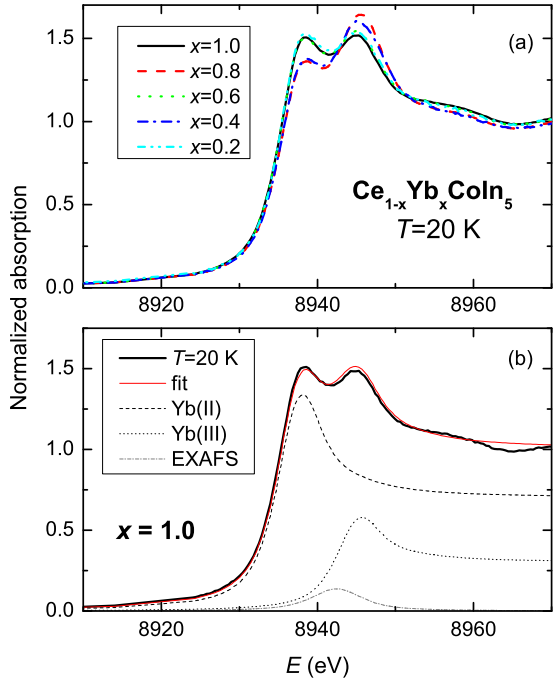

FIG. 7. (Color online) (a) Yb $L_{\rm III}$-edge XANES data at $T = 20$ K for various $Ce_{1-x}Yb_xCoIn_5$, demonstrating a small x dependence. (b) Example of a fit to extract the f-hole occupancy, n_f, in this case on $YbCoIn_5$. The individual Yb(II) and Yb(III) lineshapes consist of, essentially, a pseudo-Voigt plus an arctan function. Another pseudo-Voigt is used to roughly model the first EXAFS oscillation.

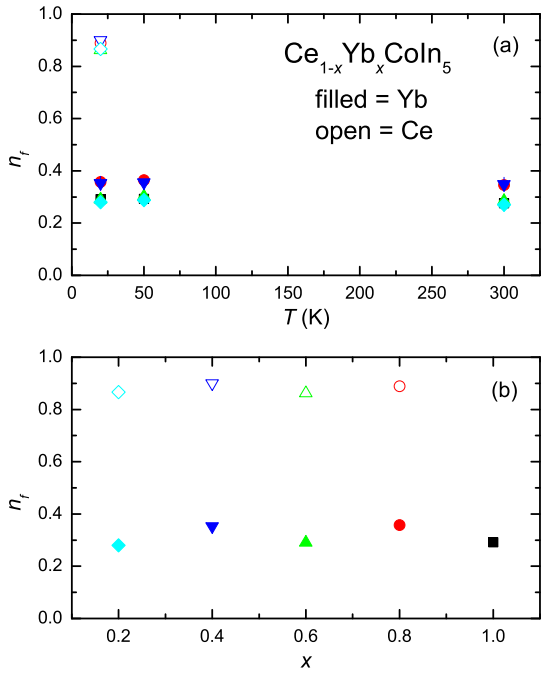

FIG. 8. (Color online) Fit results for n_f as a function of (a) temperature and (b) x, for both Ce and Yb orbitals. Note that n_f refers to the f-electron orbital occupancy for Ce, and the f-hole orbital occupancy for Yb. The rare-earth valence is then $v = n_f + 3$ for Ce and $v = n_f + 2$ for Yb.

TABLE II. Effective masses extracted from dispersions of the electron-like bands shown in Fig. 9.

$CeCoIn_5$	m^*=3.67+/-0.21	k_f=1.28 π/a
$Ce_{0.91}Yb_{0.09}CoIn_5$	m^*=4.15+/-0.32	k_f=1.31 π/a
$YbCoIn_5$	m^*=3.48+/-0.13	k_f=1.26 π/a

with the second component, which consists of the much flatter bands corresponding to either Ce f^1 spin-orbit split pair or Yb f^{14} states, respectively. The Yb f^{14} part provides the sharp f^{14} Yb peaks, seen in Figs. 10 and 11. In pure $CeCoIn_5$ the f^1 part is split by 275 meV, typical of a spin-orbit interaction, and the more localized f^0 part of the spectral intensity resides around 2.5 eV below the Fermi level, which also is typical for most Ce systems. The wider, angle-integrated scan shown in Fig. 10 shows the position, as a function of binding energy, of all the f-features of interest. The bottom of the dispersive d-band is marked as "EB". Local electronic structure at the momentum value $k = 0.9$ corresponding to the bottom of the EB band is also shown in Fig. 11.

The fitting of a parabolic dispersion to the EB band was performed in order to find the differences or system-

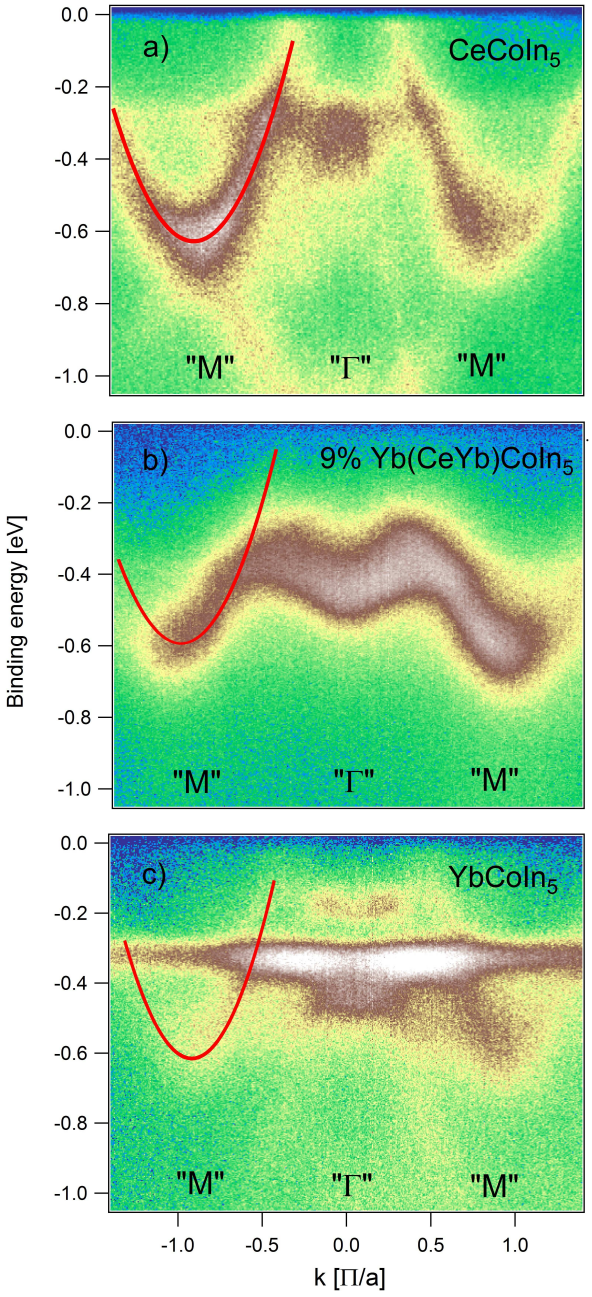

FIG. 9. (Color online) ARPES results along k_{xy} direction: comparison of the near-Fermi level electronic structure of $CeCoIn_5$, $Ce_{0.91}Yb_{0.09}CoIn_5$ and $YbCoIn_5$. For each sample, the parabolic dispersion is fitted to the characteristic electron-like feature in the conduction band (fit shown in red).

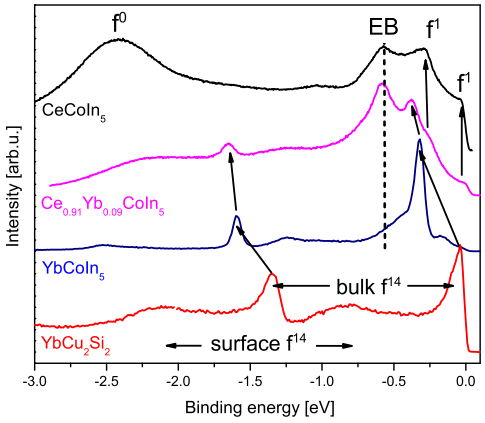

FIG. 10. (Color online) Angle-integrated electronic structure of $CeCoIn_5$, $Ce_{0.91}Yb_{0.09}CoIn_5$ and $YbCoIn_5$. The spectra for $YbCu_2Si_2$ is also shown for comparison. "EB" stands for the bottom of the electron-like band marked in red in Fig. 9.

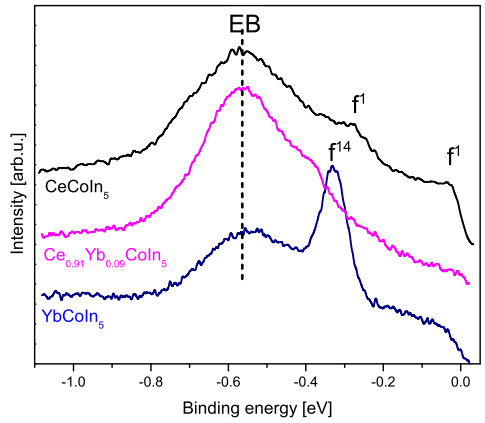

FIG. 11. (Color online) Electronic structure of $CeCoIn_5$, $Ce_{0.91}Yb_{0.09}CoIn_5$ and $YbCoIn_5$ at momentum value $k_xy = 0.9$, corresponding to the bottom of the electron-like band "EB" marked in red in Fig. 9.

atics in the electronic structure arrangement between the three samples, including the size of the electron pocket and effective mass. The effective mass extracted from this band for each compound, together with k_f values, are shown in Table II. The differences are minute (less than 20 meV, which is the instrumental resolution) and not systematic, which means the shifts are statistically not significant. We conclude that, contrary to the $CeCoIn_5$-$CeIrIn_5$-$CeRhIn_5$ family, the basic d-electron structure within the $Ce_{1-x}Yb_xCoIn_5$ series is not significantly changed with Ce-Yb substitution. Also, the Ce f^1 spin-orbit split pair is not shifted between $CeCoIn_5$ and $Ce_{0.91}Yb_{0.09}CoIn_5$, respectively, as emphasized by vertical arrows in Fig. 10.

However, the Yb-related f-electron structure is slightly modified, as indicated in Fig. 10 which shows a 50 meV shift of the Yb f^{14} structure towards higher binding energy between $YbCoIn_5$ and $Ce_{0.91}Yb_{0.09}CoIn_5$, respectively. Such shifts have been observed in strongly intermediate-valent materials. A comparison to $YbCu_2Si_2$, which has $n_f = 0.63$,[35] is also shown in

Fig. 10, to indicate the 300 meV shift in Yb f^{14} structure between $YbCu_2Si_2$ and $Ce_{0.91}Yb_{0.09}CoIn_5$, which has $n_f \approx 0.3$ from the XANES results above. The 300 meV shift therefore coincides with the difference in n_f between the two compounds of $\Delta n_f = 0.33$. A quick comparison of a few available Yb photoemission results with measured values of n_f shows that there might indeed be a correlation between the f^{14} binding energy and valence. However, we note that proper testing of this correlation and understanding the physics behind it requires a more systematic study, subject of future investigations. In the case presented here, if we simply apply the above scale of f^{14} binding energy vs. n_f, the 50 meV shift between f^{14} in $YbCoIn_5$ and $Ce_{0.91}Yb_{0.09}CoIn_5$ would correspond to $\Delta n_f = 0.055$. This small difference is consistent with the magnitude of the changes in n_f observed by XANES in Fig. 8 across the series, which are likely due to small differences in a trivalent impurity.

IV. DISCUSSION

Our main results can be summarized as follows: Yb is an intermediate-valent impurity in the $CeCoIn_5$ lattice throughout the entire doping range and the valence of both the Ce and Yb ions are stable with respect to temperature and doping. In agreement with the lack of change in the local structure, ARPES results indicate that the dispersive electron-like band is not affected by the Yb substitution. The main effect of Yb substitution is to slowly depress both T_c and γ_0.

The measured intermediate valence of $YbCoIn_5$ from the Yb $L_{\rm III}$-edge XANES is somewhat unexpected given the extremely small value of the Sommerfeld coefficient. Likewise, the magnetic susceptibility of $YbCoIn_5$ is close to zero and constant at $\chi_0 \approx 4 \times 10^{-7}$ emu/mol, after accounting for a small magnetic impurity corresponding to the low temperature Curie tail. However, the degree of intermediate valence is very high, with the lowest n_f of any non-divalent Yb intermetallic to our knowledge. For example, $YbMgCu_4$ has $n_f = 0.69$,[36] and the low temperature state of $YbInCu_4$ has $n_f = 0.83$.[37] As an order of magnitude estimate of the Kondo temperature, $T_{\rm K}$, we note that:[38]

$$T_{\rm K} = \nu\Gamma/\pi \frac{\Delta n_f}{1-\Delta n_f}, \qquad (1)$$

where ν is the magnetic degeneracy, Γ is the total hybridization strength, and Δn_f is the change in n_f at $T = 0$ K from the high-T limit, which we will assume is given by $\lim_{T\to\infty} n_f(T) = 1$. Assuming $\nu\Gamma/\pi \approx 85$ K, as in $YbAgCu_4$,[36] we find $T_{\rm K}$ is in excess of 6000 K in $YbCoIn_5$. Since $\gamma \propto \chi_0 \propto 1/T_{\rm K}$, again based on $YbAgCu_4$ results, we expect $\gamma \approx 6$ mJ mol^{-1} K^{-2} and $\chi_0 \approx 5.3 \times 10^{-4}$ emu/mol , which are consistent with the measured results given this rough estimate ($\gamma_0 = 11.6$ mJ mol^{-1} K^{-2} and $\chi_0 = 3.2 \times 10^{-7}$ emu/mol) and given the possible magnitude of the non-f contributions to the susceptibility. For instance, χ_0 in $LuAgCu_4$ is -1.5×10^{-4} emu/mol. All these data are therefore consistent with $YbCoIn_5$ being far into the intermediate-valent regime, with all the available data collected at $T << T_{\rm K}$

Lack of Fermi surface sensitivity to Yb doping is unexpected, but is in agreement with the lack of change in n_f as evidenced by the Yb $L_{\rm III}$-edge XANES results. In addition, the lack of change in n_f is consistent with the lack of change in the nearest-neighbor Yb bond lengths (Table I), although a change of up to 0.02 Å in the Yb-In pair distances may be occurring across the series. These observations support the notion that the system "does not care" if the f spectral weight is hole-like or electron-like and the symmetry arguments hold.

The main effect of Yb substitution is thus a slow depression of the superconducting transition and linear specific heat coefficient, without any significal local structural or Ce/Yb electronic structure change. This behavior is in stark contrast to the behavior from other Ce-In plane substitutions into $CeCoIn_5$, and is more similar to substitutions onto the Co site with Ir,[39] which have only a modest effect on T_c. For instance, doping onto the In sites with Cd, Sn, or Hg drives $T_c \to 0$ K after only 1.5-4% of the In is replaced, even though there is a preference for substituting into the Ce-In plane.[18,19] Perhaps a more germane comparison is to the La-doped $CeCoIn_5$ system. There, $T_c \to 0$ K after only 17% La. Like the In-site substituents, this sharp reduction has been interpreted as due to the disorder-induced unitary scattering that breaks up the Cooper pairs, as in the case of magnetic impurities in conventional superconductors.[12,18,40,41]

In contrast to these other Ce-In substitutions, and in spite of the dramatic difference between $T_{\rm K}$ of $YbCoIn_5$ and the other energy scales in the problem, such as the estimated coherence temperature $T_{\rm coh} \approx 40$ K, the strongly intermediate-valent nature of Yb in the present compounds is somehow not seen as a strong perturbation to Cooper pair formation, or even the overall electronic structure near the Fermi level. This observation therefore leads to the conclusion that the $CeCoIn_5$ and $YbCoIn_5$ networks are somehow interlaced (at least below $x \approx 0.4$ where macroscopic phase separation does not apparently occur), yet independent. In such a picture, there are at least two T_Ks (associated with each network) that affect the electronic and magnetic properties, with the overall behavior being (mostly) set from the weighted average of the two. Such an interlaced network could lead to the electronically inhomogeneous superconducting state discussed previously.[15]

Although the Ce and Yb electronic networks appear to be independent, they do have a collective effect. The similar doping dependence of both T_c and γ_0 in $Ce_{1-x}Yb_xCoIn_5$ suggests that the mechanism of Cooper pairing is closely related to the mechanism leading to large effective mass, *i.e.* the Kondo effect. One way to rationalize this relationship is that the intermediate-valent Yb neighbors *locally* change the electronic density and

thus the Kondo temperature of the Ce ions, which in turn lowers the T_c. This local electronic density change would lead to a stronger suppression of T_c than the disorder-induced pair breaking acting alone. This scenario, however, does not address the observed difference between the pair breaking due to Ce-site vs In-site substitutions. A more complete description of these effects will have a broader impact on our understanding of impurity effects in unconventional superconductors.

V. CONCLUSION

Yb $L_{\rm III}$-edge XANES measurements have established that Yb is strongly intermediate valent in $YbCoIn_5$ and across the $Ce_{1-x}Yb_xCoIn_5$ series, with an f-hole occupancy of $n_f \approx 0.3$. Such a low value of n_f implies a very low magnetic susceptibility and linear coefficient of the specific heat, as observed here and elsewhere.[31] The lack of observed changes with increasing x in the electronic structure both with XANES and ARPES measurements are consistent with previous work showing little change in other properties, notably the rather slow depression of the superconducting transition temperature.[26] This behavior is in contrast to that from all other substituents into the Ce-In plane in $CeCoIn_5$, where an Abrikosov-Gorkov-like mechanism drives $T_c \rightarrow 0$ K rapidly with x. These results therefore indicate that while Yb substitutes into the $CeCoIn_5$ lattice, the $CeCoIn_5$ network appears to act independently of the regions of $YbCoIn_5$, at least with regards to the f states, and that the heavy-fermion state preserves its coherence up to rather large doping levels. This result holds both above and below the point where macroscopic phase separation occurs, $x \approx 0.4$. Reductions in T_c and γ_0 with x are likely due to a change in the local electronic density of states near the Fermi level in the vicinity of a Yb impurity, thus altering the local Kondo interactions.

ACKNOWLEDGMENTS

We thank Eric D. Bauer for many insightful discussions. C.B. acknowledges support by the U.S. Department of Energy (DOE) under Contract No. DE-AC02-05CH11231 (Lawrence Berkeley National Laboratory). Work at LANL was performed under the auspices of the US DOE and LANL LDRD Program. The SRC is supported by the NSF under Award Np. DMR-0084402. NSF-DMR-0801253. Z.F. acknowledges support from the National Science Foundation, Grant No. NSF-DMR-0503361. X-ray absorption data were collected at the Stanford Synchrotron Radiation Lightsource, a national user facility operated by Stanford University on behalf of the DOE, Office of Basic Energy Sciences.

* Present address: Department of Physics and Astronomy, Washington State University
[1] P. W. Anderson, Phys. Rev., **124**, 41 (1961).
[2] G. R. Stewart, Rev. Mod. Phys., **56**, 755 (1984).
[3] C. M. Varma, Rev. Mod. Phys., **48**, 219 (1976).
[4] P. Pedrazzini, M. G. Berisso, N. Caroca-Canales, M. Deppe, C. Geibel, and J. G. Sereni, Eur. Phys. J. B, **38**, 445 (2004).
[5] H.-D. Kim, O. Tjernberg, G. Chiaia, H. Kumigashira, T. Takahashi, L. Duò, O. Sakai, M. Kasaya, and I. Lindau, Phys. Rev. B, **56**, 1620 (1997).
[6] J. L. Sarrao, C. D. Immer, C. L. Benton, Z. Fisk, J. M. Lawrence, D. Mandrus, and J. D. Thompson, Phys. Rev. B, **54**, 12207 (1996).
[7] E. D. Bauer, C. H. Booth, J. M. Lawrence, M. F. Hundley, J. L. Sarrao, J. D. Thompson, P. S. Riseborough, and T. Ebihara, Phys. Rev. B, **69**, 125102 (2004).
[8] S. Nakatsuji, S. Yeo, L. Balicas, Z. Fisk, P. Schlottmann, P. G. Pagliuso, N. O. Moreno, J. L. Sarrao, and J. D. Thompson, Phys. Rev. Lett., **89**, 106402 (2002).
[9] C. Petrovic, S. L. Bud'ko, V. G. Kogan, and P. C. Canfield, Phys. Rev. B, **66**, 054534 (2002).
[10] K. Izawa, H. Yamaguchi, Y. Matsuda, H. Shishido, R. Settai, and Y. Onuki, Phys. Rev. Lett., **87**, 057002 (2001).
[11] C. Petrovic, P. G. Pagliuso, M. F. Hundley, J. L. Sarrao, J. D. Thompson, and Z. Fisk, J. Phys.:Condens. Matter, **13**, L337 (2001).
[12] J. Paglione, T. A. Sayles, P.-C. Ho, J. R. Jeffries, and M. B. Maple, Nat. Phys., **3**, 703 (2007).
[13] C. Capan, Y.-J. Jo, L. Balicas, R. G. Goodrich, J. F. DiTusa, I. Vekhter, T. P. Murphy, A. D. Bianchi, L. D. Pham, J. Y. Cho, J. Y. Chan, D. P. Young, and Z. Fisk, Phys. Rev. B, **82**, 035112 (2010).
[14] Y.-f. Yang, Z. Fisk, H.-O. Lee, J. D. Thompson, and D. Pines, Nature, **454**, 611 (2008).
[15] E. D. Bauer, Y.-f. Yang, C. Capan, R. R. Urbano, M. C. F., H. Sakai, F. Ronning, M. J. Graf, A. V. Balatsky, R. Movshovich, A. D. Bianchi, A. P. Reyes, P. L. Kuhns, J. D. Thompson, and Z. Fisk, "Electronic inhomogeneity in a Kondo lattice," (2011), submitted.
[16] L. D. Pham, T. Park, S. Maquilon, J. D. Thompson, and Z. Fisk, Phys. Rev. Lett., **97**, 056404 (2006).
[17] P. Coleman, C. Pépin, Q. Si, and R. Ramazashvili, J. Phys.: Condens. Matt., **13**, R723 (2001).
[18] M. Daniel, E. D. Bauer, S.-W. Han, C. H. Booth, A. L. Cornelius, P. G. Pagliuso, and J. L. Sarrao, Phys. Rev. Lett., **95**, 016406 (2005).
[19] C. H. Booth, E. D. Bauer, A. D. Bianchi, F. Ronning, J. D. Thompson, J. L. Sarrao, J. Y. Cho, J. Y. Chan, C. Capan, and Z. Fisk, Phys. Rev. B, **79**, 144519 (2009).
[20] E. D. Bauer, F. Ronning, C. Capan, M. J. Graf, D. Vandervelde, H. Q. Yuan, M. B. Salamon, D. J. Mixson, N. O. Moreno, S. R. Brown, J. D. Thompson, R. Movshovich, M. F. Hundley, J. L. Sarrao, P. G. Pagliuso, and S. M. Kauzlarich, Phys. Rev. B, **73**, 245109 (2006).
[21] R. R. Urbano, B.-L. Young, N. J. Curro, J. D. Thompson, L. D. Pham, and Z. Fisk, Phys. Rev. Lett., **99**, 146402 (2007).

[22] A. Koitzsch, S. V. Borisenko, D. Inosov, J. Geck, V. B. Zabolotnyy, H. Shiozawa, M. Knupfer, J. Fink, B. Büchner, E. D. Bauer, J. L. Sarrao, and R. Follath, Phys. Rev. B, **77**, 155128 (2008).

[23] A. Koitzsch, I. Opahle, S. Elgazzar, S. V. Borisenko, J. Geck, V. B. Zabolotnyy, D. Inosov, H. Shiozawa, M. Richter, M. Knupfer, J. Fink, B. Büchner, E. D. Bauer, J. L. Sarrao, and R. Follath, Phys. Rev. B, **79**, 075104 (2009).

[24] H. Shishido, R. Settai, D. Aoki, S. Ikeda, H. Nakawaki, N. Nakamura, T. Iizuka, Y. Inada, K. Sugiyama, T. Takeuchi, K. Kindo, T. C. Kobayashi, Y. Haga, H. Harima, Y. Aoki, T. Namiki, H. Sato, and Y. ₋Onuki, J. Phys. Soc. Jpn., **71**, 162 (2002).

[25] D. Hall, E. C. Palm, T. P. Murphy, S. W. Tozer, Z. Fisk, U. Alver, R. G. Goodrich, J. L. Sarrao, P. G. Pagliuso, and T. Ebihara, Phys. Rev. B, **64**, 212508 (2001).

[26] C. Capan, D. Hurt, G. Seyfarth, , B. Prevost, S. Roorda, A. D. Bianchi, S. Nakasuji, and Z. Fisk, Euro. Phys. Lett., **92**, 47004 (2010).

[27] G. G. Li, F. Bridges, and C. H. Booth, Phys. Rev. B, **52**, 6332 (1995).

[28] C. H. Booth and F. Bridges, Physica Scripta, **T115**, 202 (2005).

[29] A. L. Ankudinov and J. J. Rehr, Phys. Rev. B, **56**, R1712 (1997).

[30] C. H. Booth and Y. Hu, *In Proceedings of X-Ray Absorption Fine Structure XAFS14: 14th International Conference, July 26-31, 2009*, J. Phys.: Conf. Ser., **190**, 012028 (2009).

[31] H. T. Huy, S. Noguchi, N. V. Hieu, X. Shao, T. Sugimoto, and T. Ishida, Journal of Magnetism and Magnetic Materials, **321**, 2425 (2009), ISSN 0304-8853.

[32] D. P. Rojas, L. Fernández Barquín, J. I. Espeso, J. Rodríguez Fernández, and J. Chaboy, Phys. Rev. B, **78**, 094412 (2008).

[33] M. Daniel, S.-W. Han, C. H. Booth, A. L. Cornelius, P. G. Pagliuso, J. L. Sarrao, and J. D. Thompson, Phys. Rev. B, **71**, 054417 (2005).

[34] T. Durakiewicz, P. Oppeneer, J. Wills, K. Haule, R. R. Urbano, D. Moore, E. D. Bauer, J. D. Thompson, J. J. Joyce, A. Bianchi, E. Guziewicz, J. Sarrao, and M. Butterfield, "Electronic structure tuning of the CeMIn$_5$ (M=Co, Rh, Ir) compounds," Unpublished.

[35] J. J. Joyce, A. B. Andrews, A. J. Arko, R. J. Bartlett, R. I. R. Blyth, C. G. Olson, P. J. Benning, P. C. Canfield, and D. M. Poirier, Phys. Rev. B, **54**, 17515 (1996).

[36] J. L. Sarrao, C. D. Immer, Z. Fisk, C. H. Booth, E. Figueroa, J. M. Lawrence, R. Modler, A. L. Cornelius, M. F. Hundley, G. H. Kwei, J. D. Thompson, and F. Bridges, Phys. Rev. B, **59**, 6855 (1999).

[37] A. L. Cornelius, J. M. Lawrence, J. L. Sarrao, Z. Fisk, M. F. Hundley, G. H. Kwei, J. D. Thompson, C. H. Booth, and F. Bridges, Phys. Rev. B, **56**, 7993 (1997).

[38] N. E. Bickers, D. L. Cox, and J. W. Wilkins, Phys. Rev. B, **36**, 2036 (1987).

[39] P. G. Pagliuso, R. Movshovich, A. D. Bianchi, M. Nicklas, N. O. Moreno, J. D. Thompson, M. F. Hundley, J. L. Sarrao, and Z. Fisk, Physica B, **312-313**, 129 (2002).

[40] A. A. Abrikosov and L. P. Gor'kov, Sov. Phys. JETP, **12**, 1243 (1961).

[41] E. Müller-Hartmann and J. Zittartz, Phys. Rev. Lett., **26**, 428 (1971).

DISCLAIMER